

Properties and durability of alkali-activated slag pastes immersed in sea water

Hamdy El-Didamony^a, Ahmed A. Amer^{b,*}, Hamdy Abd Ela-ziz^c

^a Faculty of Science, Chemistry Department, Zagazig University, Zagazig, Egypt

^b Faculty of Science, Chemistry Department, King Abdulaziz University, Saudi Arabia

^c National Research Center for Building and Housing, Dokki, Giza, Egypt

Received 3 October 2011; received in revised form 11 January 2012; accepted 11 January 2012

Available online 18 January 2012

Abstract

This paper represents the experimental trials to activate blast-furnace slag to produce cementless binding materials. The aims of the work is to study the properties of activated slag mixed with sodium hydroxide and sodium silicate liquid 6 wt% of granulated slag. Also, studying the effect of mixing water (tap and sea water) on the kinetic of activation. The rate of activation of the alkali activated slag (AAS) has been studied by FTIR, TGA, DTG and SEM techniques. The results revealed that the increase of NaOH content and mixing with sea water increase the combined water up to 90 days. On the other hand, the bulk density and compressive strength was increased by increasing Na₂SiO₃ content in presence of NaOH. The activated granulated slag showed good durability in sea water, i.e., the compressive strength increased gradually with immersing time up to 12 months. Whereas, the strength of sulfate resisting cement (SRC) pastes immersed in sea water increases up to 6 months then decreases up to one year. Therefore, it can be concluded that alkali activated slag are more durable in sea water than SRC pastes.

© 2012 Elsevier Ltd and Techna Group S.r.l. All rights reserved.

Keywords: Alkali-activated slag; NaOH; Na₂SiO₃; SRC; Sea water; Durability

1. Introduction

Alternative cement technologies are an area of increasing interest due to growing environmental concerns and the relative large carbon footprint of the cement industry. Many new cements have been developed, but one of the most promising is made from granulated blast furnace slag (GBFS) activated by a high-pH solution. Purdon described “the action of alkalis on slag” in 1940, but it was not until the late 1950s that the notion became widespread [1,2]. In fact, several buildings were constructed using alkali-activated slag (AAS) cements in Ukraine in the 1960s [3]. The exact nature of the activation of slag by alkalis; however, is not yet fully understood. The current status of alkali-activated materials has been spelled out in a number of recent articles [4–6]. These articles generally focus on the use of SEM/EDS, XRD, FTIR, DTA and NMR

techniques for investigating slag cement pastes. It was found that C–S–H, is the main phase produced that gives strength to Ordinary Portland Cement (OPC).

In general, an alkali-activated slag is a system in which an alkaline activator promotes one or several reactions on natural occurring solid or of an artificial origin rather than generates cementitious characteristics. The workability, durability and strength are affected by the type and concentration of the alkaline activator, solution ratio ($M_s = \text{SiO}_2/\text{Na}_2\text{O}$), slag type, fineness, curing conditions, water/cement ratio, activating solution/slag ratio and the use of admixture as well as fibers [7–10].

The behavior and durability of AAS mortars and concretes have been extensively studied [11–14]. It has been shown that they can develop comparable, and greater, mechanical strength than OPC mortars [11,12]. These materials are also highly sulfate, sea water and acid resistant [13–15]. All these properties are essentially associated with the special nature of the main hydration product which a less basic and more highly polymerized C–S–H gel than formed in OPC systems with low porosity of the mortar and concrete [16–19]. Darko

* Corresponding author. Permanent address: Faculty of Science, Zagazig University, Zagazig, Egypt. Tel.: +966 565662620.

E-mail address: drahmed.amer@yahoo.com (A.A. Amer).

and Branislav [20] examined the early hydration of alkali-slag metasilicate ($\text{Na}_2\text{SiO}_3 \cdot 5\text{H}_2\text{O}$) solution at 25 °C. The cumulative heat of hydration increases with the n modulus (n modulus of water glass means the mass ratio between SiO_2 and Na_2O). It was 3.01 with 9.62% Na_2O and 29.0% SiO_2 in this investigation. The compressive strength of AAS cements is higher than Portland cement mortars. The feasibility of using an alkaline activated ground Turkish slag to produce a mortar without Portland cement was investigated [21]. Three different activators were used: liquid sodium silicate, sodium hydroxide and sodium carbonate at different sodium concentrations.

The durability of SRC-slag blended cements in Caron's lake water was studied [22]. The results showed that the addition of blast furnace slag cement (BFSC) up to 30 wt% increases the durability and then decreases. The compressive strength of SRC pastes increases up to 6 months then decreases up to 12 months. This increase is due to the increase of the hydration of SRC with the alkali chlorides and sulfates. This increases the CSH during the first 6 months. The decrease of the strength of cement pastes up to 12 months is due to the formation and accumulation of more chloroaluminate and sulphoaluminate hydrates which cause softening as well as expansion and thereby the strength decreases.

The aim of the present investigation is to study the properties of activated slag mixed with sodium hydroxide (SH) and sodium silicate liquid (SSL) at 6 wt% of granulated slag. The mixed activator ratios are 3:3, 4:2 and 5:1 of total 6 wt% of SH and SSL of granulated slag, respectively. The effect of mixing water (tap water (TW) and sea water (SW)) on the kinetic of activation can be studied by determining the combined water, bulk density and compressive strength up to 90 days. The rate of activation of the AAS can also be studied from some selected samples by FT-IR, TGA, DTG and SEM techniques. The durability of AAS pastes in comparison with SRC immersed in SW up to one year was determined.

2. Experimental techniques

2.1. Materials

The materials used in this work are Granulated Blast Furnace Slag (GBFS) which was provided by Iron and Steel Company, Helwan Governorate, Egypt, and Sulfate Resisting Cement (SRC), provided by Helwan Portland cement company, Helwan Governorate, Egypt. NaOH was produced by SHIDO Company with purity 99%, commercial sodium silicate liquid (SSL) consists of 32% SiO_2 and 17% Na_2O with silica modulus $\text{SiO}_2/\text{Na}_2\text{O}$ equal 1.88 and density 1.46 g/cm³ was used. The granulated slag was sudden cooled by a jet of water to prevent crystallization and may be amorphous with hydraulic properties. The SRC was made from limestone, clay and iron ore to give very small amount of C_3A which is the major phase to give expansion or softening in sea water by the addition of calculated amount of iron ore to decrease the C_3A content to 3% and increase C_4AF which has good durability [23].

The chemical composition of the starting materials is shown in Tables 1 and 2.

Table 1

Chemical composition of starting materials (wt%).

Oxide, %	SiO_2	Al_2O_3	Fe_2O_3	CaO	MgO	SO_3	Na_2O	K_2O	L.O.I.
GBSF	37.81	13.14	0.23	38.70	7.11	1.19	1.03	0.19	–
SRC	20.85	4.63	5.38	63.15	2.03	1.56	0.22	1.21	1.89

Table 2

The chemical analysis of the seawater.

Test	pH	Cl^-^a	$\text{SO}_4^{2-}{}^a$	$\text{Ca}^{2+}{}^a$	$\text{Na}^+{}^a$	$\text{K}^+{}^a$	$\text{Mg}^{2+}{}^a$	TDS ^b
Sea W	8.13	22,300	1450	210	11,520	477	1341	43,300

^a ppm unit.

^b Total dissolved solids.

Fig. 1 illustrates the XRD pattern of Granulated Blast Furnace Slag. It is clear that the GBFS is nearly completely vitreous with an amorphous structure.

The GBFS was firstly crushed in a jaw crusher to pass through a 2 mm diameter sieve, then passed through a magnet to remove any contamination of iron melt then ground in steel ball mill to reach $4500 \pm 50 \text{ cm}^2/\text{g}$ surface area. Mixes were prepared from granulated slag using mixed activator as shown in Table 3. The pastes were prepared using sodium hydroxide NaOH (SH) and sodium silicate liquid Na_2SiO_3 (SSL) as activators at 6 wt% of dry mixes. In an earlier work [24] it was found that 6 wt% of NaOH is the optimum amount for the activation of slag. The slag was mixed with sea or tap water then cured in 100% R.H. The water to binder ratio (w/b) is 0.26.

2.2. Preparation of pastes

Ground granulated slag was placed on smooth, non-absorbent surface, a crater was formed in the center and the mixing water at 0.26 with the activator was poured into the crater. The water of consistency of granulated slag was determined according to ASTM specification [25]. The mixture was slightly troweled to absorb the water for about 1 min, then completed by vigorous mixing for 3 min. The paste was moulded in one inch cubic moulds, then strong manually

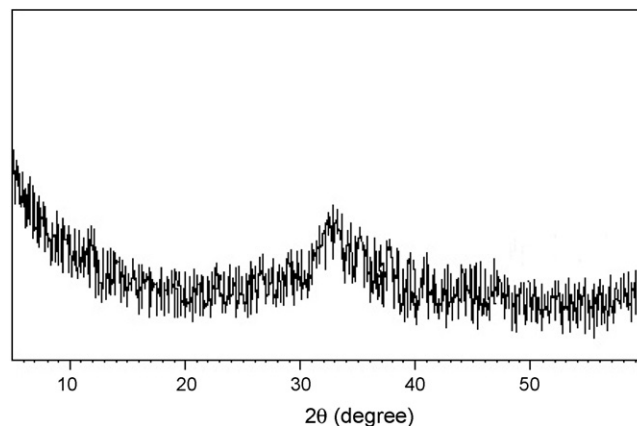


Fig. 1. XRD pattern of granulated blast furnace slag sample.

Table 3

Composition of the investigated mixes, wt%.

Mix. no.	GBFS	SH:SSL, %	Type of mixing water
I. 1	100	3:3	TW and SW
I. 2	100	4:2	TW and SW
I. 3	100	5:1	TW and SW

pressed into the moulds. The surface of the paste was then smoothed by thin edged trowel.

Immediately after moulding, the specimens were cured in 100% R.H. at room temperature 23 ± 2 °C for 24 h, then demoulded and cured in the humidifier up to 3, 7, 28 and 90 days. For the durability of the slag as well as SRC pastes in sea water, the pastes were cured up to 28 days (zero time) in 100% R.H. then immersed in sea water up to 1, 3, 6, 9 and 12 months.

The combined water is used as an indication for the degree of hydration of the pastes. The hydration was stopped by drying the pastes at 105 °C for 24 h, then kept in air-tight bottles till testing. The combined water content was determined from the ignition of the dried paste at 800 °C for 20 min.

The water of consistency of SRC was 0.28. The bulk density and compressive strength were determined as described elsewhere [26,27].

Thermal gravimetric analysis (TGA) was carried out using DTA-50 Thermal Analyzer (Schimadzu Co., Tokyo, Japan). A dried sample of about 50 mg (-53 μ m) was used at heating rate 20 °C/min under nitrogen atmosphere. For IR spectroscopic investigation, the samples were prepared using alkali halide KBr pressed disk technique [28]. The IR analysis was recorded from KBr disks using Gensis FT-IR spectrometer in the range 400–4000 cm^{-1} after 256 scans at 2 cm^{-1} resolution.

The scanning electron microscope (SEM) was taken with *Inspect S* (FEI Company, Holland) equipped with an energy dispersive X-ray analyzer (EDX). SEM was used to examine the microstructure of the fractured composites at the accelerating voltage of 200–30 kV and Power zoom magnification up to 300,000 \times . The samples are firstly dried at 105 °C until constant weight, then, bonded on the sample holders with conducting glue carbon. The morphologies of the products are observed at microscopic level.

3. Results and discussion

3.1. Activation of granulated slag by sodium hydroxide (SH) and sodium silicate (SSL) cured at 100% R.H.

The activation of granulated slag was determined by determining the combined water content, bulk density and compressive strength of activated slag up to 90 days. Some selected samples were investigated with FT-IR, thermal analysis, DTA and SEM. Also, the durability of activated granulated cement in comparison with commercial sulfate resisting cement (SRC) pastes immersed in sea water up to one year was carried out.

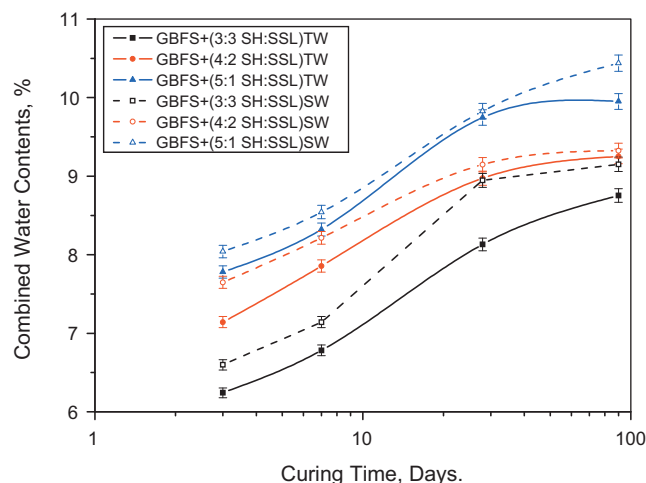


Fig. 2. Combined water contents of activated slag mixed with sea or tap water then cured in 100% R.H.

3.1.1. Chemically combined water

Chemically combined water contents of activated slag mixed with tap or sea water and cured in 100% R.H. up to 90 days are graphically plotted in Fig. 2. It is clear that the combined water contents of activated slag pastes gradually increases up to 90 days. This is due to the continuous hydration and accumulation of hydrated products in some of open pores that increase the combined water. Also, the combined water contents of pastes mixed with sea water are higher than those mixed with tap water. This is due to the presence of some alkali soluble salts such as sodium, potassium, magnesium, calcium ions, etc. in sea water which can activate and increase the combined water contents.

3.1.2. IR spectroscopy

IR shows absorption bands at 1094, 800, 600 and 470 cm^{-1} , characteristic of the four co-ordinated silica and the first two bands due to the symmetric stretching. They shifted to lower frequency which arise from increasing contribution made by Si–O–Al linkage [29]. Crystalline silica and crystobalite revealed strong absorption bands at 1200 and 800 cm^{-1} arising from silicon oxygen fundamental, two forms of bonding Si–O bond or siloxan group, and Si–OH bond or silanol group. Si–O bond gives a characteristic band due to bending vibration at 400–500 cm^{-1} and stretching vibration band between 800 and 1000 cm^{-1} the silica tetrahedral connected to form chains or more complicated structure, occurs mainly at absorption bands 470, 600, 810 and 1100 cm^{-1} . The absorption bands at 1635 and 3460 cm^{-1} are of water molecules adsorbed on the silica form [30].

Fig. 3 represents the IR-spectra of anhydrous and activated slag with (3:3 SH and SSL, %) mixed with tap water and cured in humidity for 3 and 90 days. The IR spectra of anhydrous GBFS, give two main bands at 492 and 988 cm^{-1} as well as two less intense bands at 717 and 1422 cm^{-1} . Bands at 988 and 492 cm^{-1} imply the presence of orthosilicate unit $[\text{Si}_2\text{O}_7]^{6-}$ with partial substitution of Si^{4+} by Al^{3+} in tetrahedral positions. These units are built of two silicoxygen (or silico/and

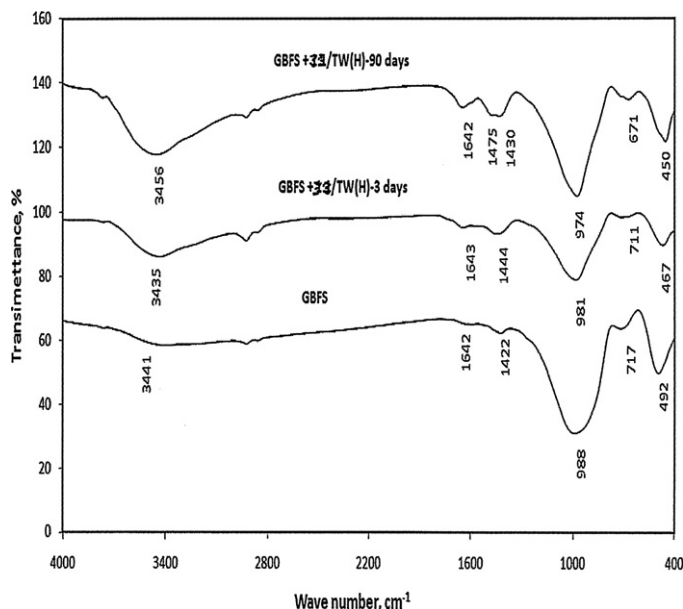


Fig. 3. FTIR-spectra of anhydrous GBFS and activated GBFS with (3:3 SH, SSL, wt%) mixed with tap water then cured in humidity for 3 and 90 days.

aluminooxygen) tetrahedral, connected with oxygen bridge. These two bands represent the internal vibrations for $[\text{SiO}_4]^{4-}$ and $[\text{AlO}_4]^{5-}$ tetrahedral [31]. The first comes from Si(Al)–O anti symmetric stretching vibrations; the second should be assigned to bending vibration of O–Si–O bonds [32]. The appearance of the most intense band at relative low wave numbers proves the silicate phases in the slag containing orthosilicate units $[\text{Si}_2\text{O}_7]^{6-}$. The existence of the weak band at 716 cm^{-1} , assigned to the symmetric stretching vibration of the Si–O–Si(Al) bridges, which confirms the presence of these units. It is also possible to support this by ageing that the Si–O–Al bridges can also result from linkage between $[\text{SiO}_4]^{4-}$ and $[\text{AlO}_4]^{5-}$ tetrahedral [33]. Moreover, it is impossible to exclude the association of this band with Al–O vibrations, appearing in aluminosilicates octahedral. High content of aluminum shifts the band 988 cm^{-1} at such low wave number. Aluminum atoms in tetrahedral coordination influence a shift of the most intense band to lower wave numbers, in relation to 1100 cm^{-1} position characteristic for pure silica spectra in non-hydrated form [34]. Low intensity bands at 1422 cm^{-1} originates from carbonate groups $[\text{CO}_3]^{2-}$. High full width at half maximum (FWHM) especially in the case of most intense band at 988 cm^{-1} proves the significant content of glassy phase in the slag. It is known that the phases of non-ordered structure increase the band width due to the existence of significant fluctuations of geometric parameter. The shape of the spectra is typical of glassy aluminosilicates belonging to the groups of gehlenites and melilites [35].

The IR spectra of the activated slag with (3:3 SH and SSL) mixed with tap water and cured in humidity for 3 and 90 days revealed that, the main absorption bands which is related to Si–O(Al) anti symmetric stretching vibration in case of (GBFS) at 988 cm^{-1} is shifted to 981 cm^{-1} as well as 972 cm^{-1} with decrease in width of the bands, respectively at 3 and 90 days. This fact should be related to the increase of crystallinity of the

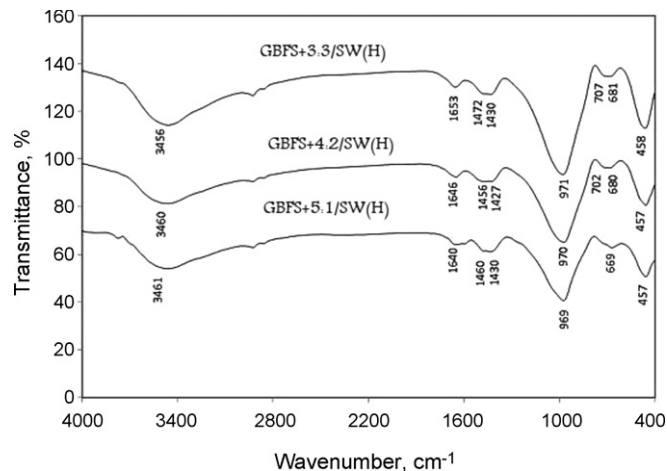


Fig. 4. FTIR spectra of GBFS pastes activated with (3:3, 4:2 and 5:1 SH:SSL, wt%) mixed with sea water and cured in humidity at 90 days.

sample caused by ordering of the structure. Absorption bands at $1642\text{--}1643\text{ cm}^{-1}$ and at $3435\text{--}3456\text{ cm}^{-1}$ are related to bending vibration of H:OH and stretching of O–H groups, respectively. Absorption bands of water are due to lattice H_2O of the hydrated C–S–H, C–A–H as well as C–A–S–H. These values confirmed the formation of the geo-polymer [36]. Absorption bands at $1422\text{--}1475\text{ cm}^{-1}$ are assigned to atmospheric carbonation. Bands at $671\text{--}717$ and $450\text{--}492\text{ cm}^{-1}$ which are related to symmetric stretching vibrations of the Si–O–Si (Al) bridges and O–Si–O bending vibrations have high intensity and low of (FWHM) than those of 3 days activated sample and GBFS at $711\text{--}717\text{ cm}^{-1}$. This is due to the increase of geo-polymer formation and also the glassy phase of the sample. It was stated that the structure of AAS phases is a transition between the structures of Ordinary Portland Cement and geo-polymers [37].

Fig. 4 illustrates the FTIR-spectra of granulated slag activated with 3:3, 4:2 and 5:1(SH:SSL) mixed with sea water and cured for 90 days. The individual bands of activated slag are identical but with slight intensity differences and (FWHM) of the bands. The intensity of bands at $457\text{--}458\text{ cm}^{-1}$ due to O–Si–O bending vibration, absorption bands $669\text{--}707\text{ cm}^{-1}$ related to symmetric stretching vibrations of the Si–O–Si (Al) bridges. This band at $969\text{--}971\text{ cm}^{-1}$ related to Si(Al)–O anti symmetric stretching vibration. The intensity of bands at $1640\text{--}1653$ and $3456\text{--}3461\text{ cm}^{-1}$ assigned to bending vibration of H:OH and stretching of O–H group of activated slag with 3:3 are greater than that activated with 4:2 and 5:1(SH:SSL). This is due to that at low alkalinity (3:3 SH:LSS), dissolution of calcium from granulated slag occurs to form C–S–H conjunction with the geo-polymeric gel. But at high alkalinity (4:2 and 5:1 SH:SSL), the dissolution of Ca^{2+} increases forming $\text{Ca}(\text{OH})_2$ which precipitates on the activated slag then lowers the alkalinity of the medium. Therefore, the activation decreases with SH content [38]. Also, the (FWHM) decreases with SSL content due to the fact that the degree of crystallinity of slag pastes increases with SSL content. The short absorption bands at $1427\text{--}1472\text{ cm}^{-1}$ are due to atmospheric carbonation.

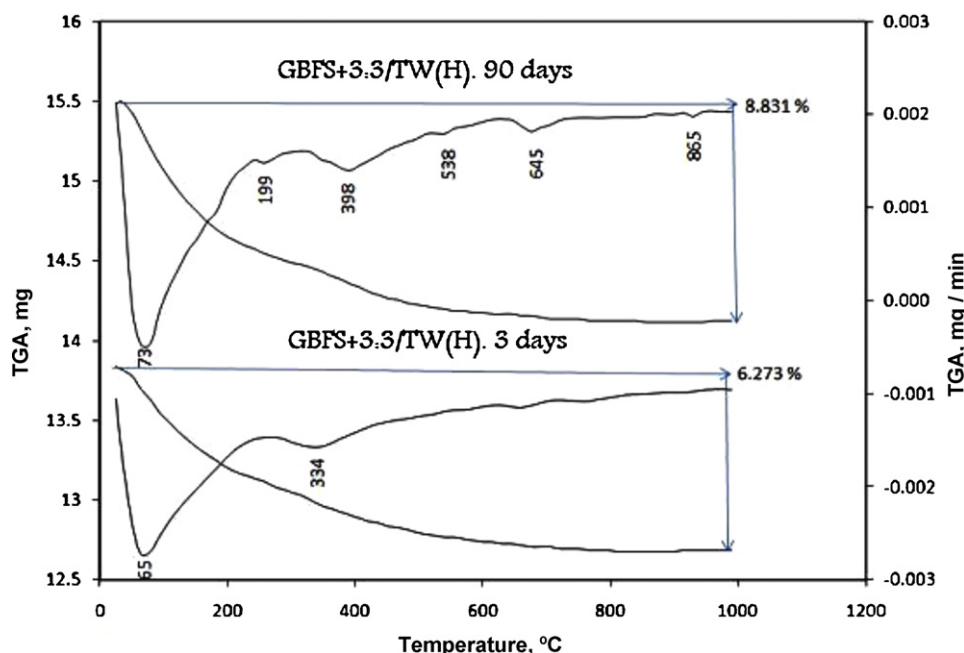


Fig. 5. TGA and DTG of activated slag pastes with (3:3 SH:SSL) mixed with tap water and cured in humidity for 3 and 90 days.

3.1.3. Thermo gravimetric analysis

Fig. 5 presents TGA and DTG of activated slag with (3:3 SH:SSL) mixed with tap water and cured for 3 and 90 days. The weight loss at 1000 °C was found to be 6.273% and 8.831% for 3 and 90 days, respectively. Endotherms at 65 and 73 °C are due to the dehydration of free water and C–S–H from hydrated matrix [39]. The endothermic peaks at 199, 334 and 398 °C related to C–A–S–H and C–A–H [40]. The endotherm at 655 °C related to the decomposition of carbonate, hydrated aluminates and final stage of decomposition of C–S–H [29]. Endothermic peak at 865 °C is due to the decomposition of well crystallized CaCO_3 .

3.1.4. Scanning electron microscopy (SEM)

The SEM of hardened activated slag mixed with (3:3 SH:SSL) and sea water for 3 and 90 days are shown in Fig. 6A–D. It is found that, the microstructure of activated slag by (3:3 SH:SSL) for 90 days displayed compaction of matrix structure with the presence of highly crystalline geopolymer (GP). This fills some of the pores as shown in Fig. 6C, and compared to the less dense structure at 3 days (Fig. 6A). While, the EDX analysis (Fig. 6B) of activated slag for 3 days indicates the presence of alumina, silica and oxygen which form the GP. It also contain calcium and silica which form CSH. On the other hand, the SEM micrograph of activated slag by (5:1 SH:SSL) for 90 days shows poorly crystalline structure of hydration and GP products than those activated by (3:3 SH:SSL) which has a highly crystalline structure. This is due to fact that the SSL increases the amount of $[\text{SiO}_4]^{4-}$ in the medium which reacts with Al and Si forming geopolymer [20]. This GP forms long chains which react with each other producing very compact structure as shown in Fig. 6C. The reaction products of alkali-activated materials are different depending on the calcium content of the activated material.

The alkaline activation of calcium-free materials such as metakaolin and some fly ashes forms amorphous to semi crystalline three-dimensional aluminosilicate networks by polycondensation [41]. These binders are also known as “geopolymers” [42].

3.1.5. Bulk density

Bulk density of hardened activated slag mixed with tap or sea water up to 90 days is plotted in Fig. 7. It is clear that the bulk density of AAS mixed with sea water is higher than that mixed with tap water due to the presence of some salts which accelerate the hydration. The bulk density of AAS increases with curing time due to the continuous activation and formation of hydrated products. These are deposited in the open pores that increase the density of the activated slag. The increase of SSL enhances the bulk density of the paste. The dispersed medium contains higher concentration of $[\text{SiO}_4]^{4-}$ which increases the rate of hydration and formation of more C–S–H and C–A–S–H that enhance the bulk density.

3.1.6. Compressive strength

The compressive strength of activated granulated slag mixed with tap or sea water up to 90 days is graphically represented in Fig. 8. The compressive strength of activated slag increases up to 90 days. The compressive strength of hardened slag mixed with sea water is higher than that mixed with tap water due to the activation of the alkali salts like NaCl, MgCl_2 , Na_2SO_4 and MgSO_4 which accelerate the activation. Also, the compressive strength increases with the SSL content which contains high concentration of $[\text{SiO}_4]^{4-}$ that increases the reaction with Ca^{2+} to form C–S–H or with Si^{4-} and Al^{3+} to form Si–O–Si, Al–O–Si geo-polymer [20]. The compressive strength is in a good agreement with TGA/DTG analysis.

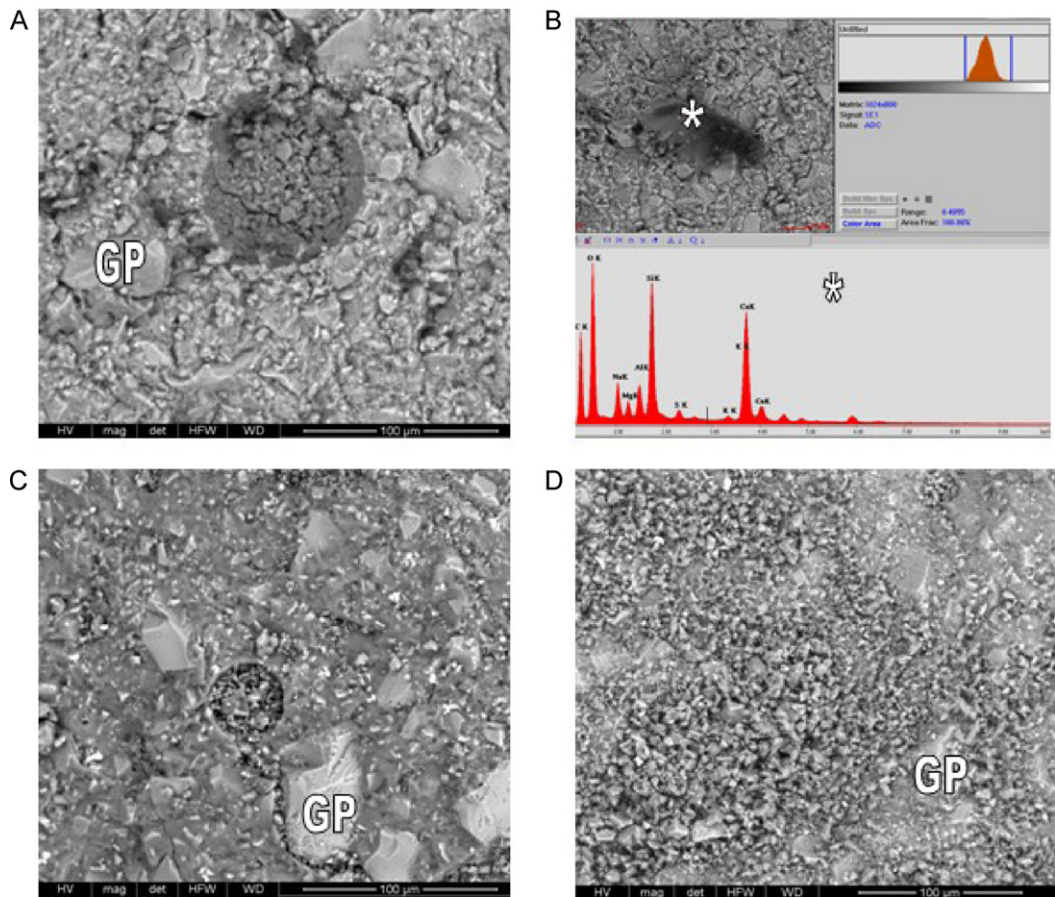


Fig. 6. SEM of slag [(A) activated with (3:3 SH:LSS) at 3 days, (B) its EDX, (C) activated with (3:3 SH:SSL) and (D) activated with (5:1 SH:SSL)] mixed with sea water for 90 days.

3.1.7. Durability in sea water

The compressive strength of activated granulated slag as well as SRC mixed and immersed in sea water up to one year is graphically plotted in Fig. 9. The high strength of SRC pastes at zero time is due to its higher rate of hydration compared to granulated slag. It is clear that the compressive strength of activated slag increases up to one year. Alkali activated slag can

lead to good durability and high resistance to chemical attack. This is due to the continuous activation of granulated slag forming CSH as well as CASH [5]. Also, as the amount of Na_2SiO_3 increases the strength also increases. The compressive strength of SRC pastes immersed in sea water increases up to 6 months then decreases up to 12 months [22,43]. The increase of strength is due to the continuous activation by sea water

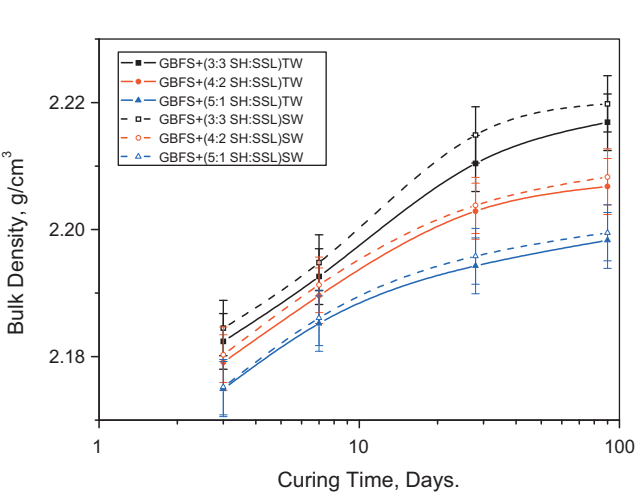


Fig. 7. Bulk density of activated slag mixed with sea or tap water then cured up to 90 days.

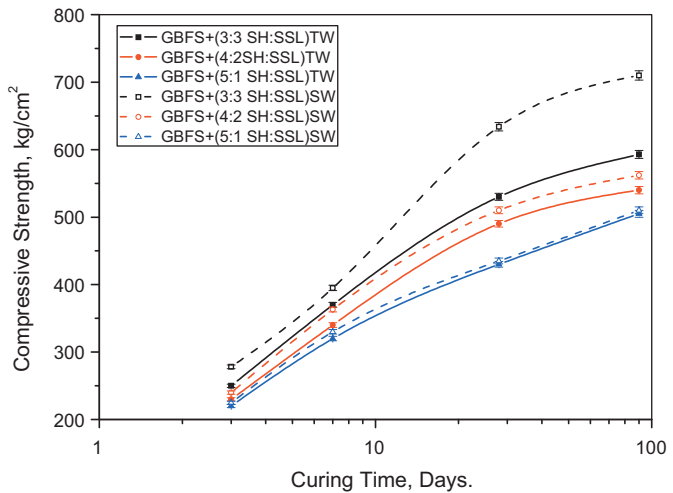


Fig. 8. Compressive strength of activated slag mixed with sea or tap water up to 90 days.

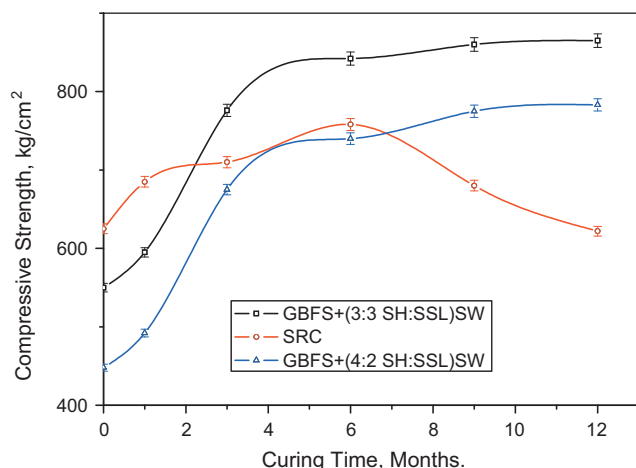


Fig. 9. Compressive strength of activated GBFS and SRC pastes mixed with sea water then immersed in sea water up to one year.

forming more CSH. Whereas, the decrease of strength of SRC pastes after 6 months is mainly due to the presence of high values of alite and belite which liberate $\text{Ca}(\text{OH})_2$ that forms ettringite as well as Friedel salt [40–44]. These phases expand or soften the cement pastes. By comparing the AAS with SRC, it is found that the strength of AAS increases up to 12 months due to the formation of CSH and geo-polymer [36,40] with the absence of chloroaluminate and ettringite.

4. Conclusion

The main conclusions could be derived from this investigation are summarized as follows:

1. The mixed activators (SH/SSL) give more suitable properties than those of only NaOH.
2. The increase of NaOH content on the expense of Na_2SiO_3 shows higher combined water contents but lower bulk density and compressive strength. The increase of compressive strength is due the increase of $[\text{SiO}_4]^{4-}$ which enhances the CSH formation. On the other hand, the increase of NaOH increases the combined water content.
3. The alkali activation of slag with NaOH and Na_2SiO_3 can be used as cementing materials in sea water environment, with higher durability.
4. The sulfate resisting cement (SRC) can not be used as sea water resisting cement due to the presence of C_3S and $\beta\text{-C}_2\text{S}$ which liberates $\text{Ca}(\text{OH})_2$ which is the main source of ettringite as well as chloroaluminate hydrates formation.

Acknowledgments

We acknowledge with pleasure the Deanship of Scientific Research (DSR), King Abdulaziz University, Jeddah, Saudi Arabia for the continuous support of such project No. 388/372/1431.

The authors are also grateful to thank Dr. A.A. Amer, Assoc. Prof., Faculty of Science, Zagazig University for his great help throughout the interpretation of the results of this article.

References

- [1] F. Pacheco-Torgal, J. Castro-Gome, S. Jalali, Alkali activated binders: a review. Part I: Historical background, terminology, reaction mechanisms and hydration products, *Constr. Build. Mater.* 22 (2008) 1305–1314.
- [2] D.M. Roy, Alkali activated cements. Opportunities and challenges, *Cem. Concr. Res.* 29 (1999) 249–254.
- [3] H. Xu, J.L. Provis, J.S.J. van Deventer, P.V. Krivenko, Characterization of aged slag concretes, *ACI Mater. J.* 105 (2008) 131–139.
- [4] F. Pacheco-Torgal, J. Castro-Gomes, S. Jalali, Alkali activated cements: a review. Part 2. About materials and binders manufacture, *Constr. Build. Mater.* 22 (2008) 1315–1322.
- [5] P. Duxson, A. Fernández-Jiménez, J.L. Provis, G.C. Lukey, A. Palomo, J.S.J. van Deventer, Geopolymer technology: the current state of the art, *J. Mater. Sci.* 42 (2007) 2917–2933.
- [6] C. Shi, P.V. Krivenko, D.M. Roy, Alkali-activated Cements and Concretes, Taylor and Francis, Abingdon, UK, 2006.
- [7] A. Fernandez-Jimenez, F. Puertas, Effect of activator mix on the hydration and strength behavior of alkali-activated slag cements, *Adv. Ceram. Res.* 15 (2003) 129–136.
- [8] M. Ben Hafa, G. Le Saout, F. Winnefeld, B. Lothenbach, Influence of activator type on hydration kinetics, hydrate assemblage and microstructural development of alkali-activated blast-furnace slags, *Cem. Concr. Res.* 41 (2011) 301–310.
- [9] E. Rodriguez, S. Bernal, R. Mejia de Gutierrez, Y.F. Puertas, Alternative concrete based on alkali-activated slag, *Mater. De Constr.* 58 (291) (2008) 53–67.
- [10] M. Palacios, Y.F. Puertas, Effect of superplasticizer and shrinkage-reducing admixtures on alkali-activated slag pastes and mortars, *Cem. Concr. Res.* 35 (2005) 1358–1367.
- [11] V.D. Glukhovskiy, G.S. Rostovskaja, G.V. Rumyna, High strength slag-alkaline cements, in: 7th International Congress Chemistry Cement (Paris), vol. 3, 1980, 164–168.
- [12] S.A. Bernal, R. Mejia de Gutierrez, A.L. Pedraza, J. Provis, Effect of binder content on the performance of alkali-activated slag concretes, *Cem. Concr. Res.* 41 (2011) 1–8.
- [13] T. Bakharev, J.G. Sanjayan, Y.B. Cheng, Sulfate attack on alkali-activated slag concrete, *Cem. Concr. Res.* 32 (2002) 211–216.
- [14] F. Puertas, R. Mejia de Gutierrez, A. Fernandez-Jimenez, S. Delvasto, J. Maldonado, Alkaline cement mortars, chemical resistance to sulphate and seawater attack, *Mater Construc.* 52 (267) (2002) 55–71.
- [15] T. Bakharev, J.G. Sanjayan, Y.B. Cheng, Resistance of alkali-activated slag concrete to acid attack, *Cem. Concr. Res.* 33 (2003) 1607–1611.
- [16] J.I. Escalante-Garcia, A.F. Fuentes, A. Gorokovskiy, P.E. Fraire-Luna, G. Mendoza-Suarez, Hydration products and reactivity of blast-furnace slag activated by various alkalis, *J. Am. Ceram. Soc.* 86 (12) (2003) 48–53.
- [17] A. Fernandez-Jimenez, F. Puertas, I. Sorbrados, J. Sanz, Structure of calcium silicate hydrates formed in alkaline activated slag. Influence of the type of alkaline activator, *J. Am. Ceram. Soc.* 86 (8) (2003) 1389–1394.
- [18] F. Puertas, A. Fernandez-Jimenez, M.T. Blanco-Varela, Pore solution in alkali-activated slag cement pastes. Relation to the composition and structure of calcium silicate hydrate, *Cem. Concr. Res.* 34 (2004) 139–148.
- [19] C. Shi, Strength, pore structure and permeability of alkali-activated slag mortars, *Cem. Concr. Res.* 26 (1996) 1789–1799.
- [20] K. Darko, Z. Branislav, Effects of dosage and modulus of water glass on early hydration of alkali-slag cements, *Cem. Concr. Res.* 32 (2002) 1181–1188.
- [21] D. Atis Cengiz, C. Bilim, C. Özlem, K. elik Okan, Influence of activator on the strength and drying shrinkage of alkali-activated slag mortar, *Constr. Build. Mater.* 23 (2009) 548–555.
- [22] M. Abd El-Aziz, S. Abd El-Aleem, M. Heikal, H. El-Didamony, Hydration and durability of sulphate-resisting and slag cement blends in Caron's lake water, *Cem. Concr. Res.* 35 (8) (2005) 1592–1600.
- [23] P.C. Hewlett, Lea's Chemistry of Cement and Concrete, 3rd ed., John Wiley & Sons Inc., New York, 1998.

- [24] M.S. Hafeez, Preparation and characterization of the non Portland Cement, M.Sc. thesis, Faculty of Science, Zagazig University, Zagazig, Egypt, 2008.
- [25] ASTM Designation: C-191, Standard method for normal consistency and setting of hydraulic cement, ASTM Annual Book of ASTM Standards, 04.01, 2008.
- [26] H.H. Assal, Some studies on the possibility of utilization of calcareous shale/clay deposits in building bricks industry, Ph.D. thesis, Faculty of Science, Zagazig University, Zagazig, Egypt, 1995.
- [27] ASTM C109M, Standard test method for compressive strength of hydraulic cement mortars, 2007.
- [28] R.J. Errington, Advanced Practical Inorganic and Metal Organic Chemistry, Balckie Academic Professional, An Impient Chapman & Hall, 1997.
- [29] N.Y. Mostafa, S.A.S. El-Hemaly, S.A. El-Wakeel, P.W. Brown, Characterization and evaluation of the hydraulic reactivity of water-cooled slag and air cooled slag, *Cem. Concr. Res.* 31 (2001) 899–904.
- [30] D.M. Ibrahim, S.A.S. El-Hemaly, E.A. Abdel-Karim, Study of rice husk ash silica by infrared spectroscopy, *Thermochim. Acta* 37 (1981) 307–314.
- [31] M. Criado, A. Fernandez-Jimenez, A. Palomo, Alkali-activation of fly ash: effect of the $\text{SiO}_2/\text{Na}_2\text{O}$ ratio. Part I: FTIR study, *Microporous Mesoporous Mater.* 106 (2007) 180–191.
- [32] M. Handke, *Appl. Spectrosc.* 40 (1986) 871.
- [33] K. Ishida, D.M. Jenkins, F.C. Hawthorne, *Am. Mineral.* 93 (2008) 1112.
- [34] J. Zhang, J.L. Provis, D. Feng, J.S.J. van Deventer, Geopolymers for immobilization of Cr^{6+} , Cd^{2+} , and Pb^{2+} , *J. Hazard. Mater.* 157 (2/3) (2008) 587–598.
- [35] G.E. De Benedetto, R. Laviano, L. Sabbatini, P.G. Zambonin, Infrared spectroscopy in the mineralogical characterization of ancient pottery, *J. Cult. Heritage* 3 (3) (2002) 177–186.
- [36] T. Bakharev, Durability of geopolymer materials in sodium and magnesium sulfate, *Cem. Concr. Res.* 35 (6) (2005) 1233–1246.
- [37] I. Lecomte, C. Henrist, M. Liegeois, F. Maseri, A. Rulmont, R. Cloots, Micro-structural comparison between geopolymers, alkali-activated slag cement and portland cement, *J. Eur. Ceram. Soc.* 26 (2006) 3789–3797.
- [38] J. Davidovits, in: J. Davidovits (Ed.), *Proceedings of the Second International Conference Geopolymer'99*, St. Quentin, France, (1999), p. 9.
- [39] J. Davidovits, *IUPAC International Symposium on Macromolecules. Topic III New Polymers of High Stability*, Stockholm, 1976.
- [40] K. Yip Christina, C. Lukey Grant, L. Provis John, S.J. Van Deventer Jannie, Effect of calcium silicate sources on geopolymerization, *Cem. Concr. Res.* 38 (2008) 554–564.
- [41] K. Garbev, Structure, properties and quantitative rietveld analysis of calcium silicate hydrates (C–S–H phases) crystallised under hydrothermal conditions, PhD thesis, Institut für Technische Chemie von der Fakultät für Chemie und Geowissenschaften der Ruprecht-Karls-Universität Heidelberg, Germany, June 2004.
- [42] H.F.W. Taylor, *Cement Chemistry*, 2nd ed., Thomas Telford Publication, London, 1998.
- [43] I.M. Helmy, A.A. Amer, H. El-Didamony, Chemical attack of hardened pastes of blended cements. Part I: attack of chloride solutions, *ZKG 44* (2) (1991) 46–50.
- [44] H. El-Didamony, A.A. Amer, I.M. Helmy, K. Mostafa, Durability of sulphate resisting blended cements and mortars in sea water, *Indian J. Technol.* 3 (1996) 35–40.